

Mixed-Valence Polyvanadic Acid Gels

N. GHARBI, C. SANCHEZ, J. LIVAGE,* J. LEMERLE, L. NÉJEM, and J. LEFEBVRE

Received April 6, 1981

Polyvanadic acid gels are made by polymerization of decavanadic acid. High-condensed species are obtained ($M_r \approx 2 \times 10^6$), and electron microscopy shows that the gel is made of entangled fibers. ESR and light-scattering experiments suggest that polyvanadic acid colloids are polydispersed coils rather than rods as previously mentioned. Some vanadium reduction occurs during the polymerization process in water leading to a mixed-valence polymer. Layers can easily be deposited from the gel on a glass substrate. They exhibit semiconducting properties arising from the hopping of unpaired electrons between V(IV) and V(V) ions. The measured dc conductivity of these layers is surprisingly high ($\sigma \approx 0.6 \Omega^{-1} \text{ cm}^{-1}$ at 300 K). The transfer integral J between vanadium sites has been evaluated from measurements of the optical and thermal activation energies for hopping. A value of $J \approx 0.05 \text{ eV}$ is found, showing that polyvanadic acid gels belong to the mixed-valence compound class II. ESR and visible-UV spectroscopy suggest the existence of hexacoordinated VO^{2+} vanadyl ions in a C_{4v} ligand field. A water molecule is presumably directly bound to the metal ion on the sixth position opposite to the $\text{V}=\text{O}$ double bond.

Introduction

Vanadium pentoxide gels have been known for a long time.¹⁻⁴ They can be obtained by adding nitric acid to a vanadate salt¹ or by pouring molten V_2O_5 into water.⁴ Hydrolysis of vanadic esters also leads to colloidal solutions.³ Nevertheless, very few studies have actually been published during the last decade. Most of them dealt with the optical and hydrodynamic properties of vanadium pentoxide hydrosols.⁵⁻⁷ Donnet et al.⁵ have related the vanadium concentration dependence of the optical absorption with the fixation of colored ions at the surface of the colloid. Such ions were supposed to be easily hydrolyzed into colorless ions. Vanadium pentoxide sols have also been chosen as a model in order to study the hydrodynamic behavior of rigid particle suspensions.⁵ The effect of small quantities of OH^- or H_3O^+ ions, together with the aging of the sols, was followed by viscosity measurements, but no suitable explanation was found,⁸ presumably because of the presence of foreign ions in the sol.

This paper deals with vanadium pentoxide gels obtained by polymerization of vanadic acid.⁹ Such a procedure yields pure polyvanadic acid gels free of foreign ions such as Na^+ or NO_3^- . The physicochemical properties of these gels will first be presented in order to determine the chemical nature and the polymeric structure of the macromolecular species.

Some reduction occurs during the polymerization process. A class II mixed-valence compound is thus obtained, the semiconducting properties of which arise from the hopping of unpaired electrons between V(IV) and V(V) ions.¹⁰ ESR, optical spectroscopy, and electrical conductivity measurements are also presented in order to obtain information about vanadium coordination and electron delocalization in the polyvanadic acid gels.

Experimental Section

Polyvanadic acid solutions are prepared by ion exchange in a resin (Dowex 50W-X2, 50-100 mesh) from sodium metavanadate solutions.⁹ The freshly prepared acid is yellow and decacondensed. High polymers are spontaneously formed through an autocatalytic process. Colloidal solutions become dark red, and their viscosity increases upon aging. Gelation occurs for a vanadium concentration greater than 0.1 mol L^{-1} . No change is observed after 15 days, and all measurements have been performed on such aged polyvanadic colloidal solutions or gels.

Vanadium titrations were carried out by atomic absorption measurements in a nitrous oxide-acetylene flame, with a Perkin-Elmer spectrophotometer (Model 392). V(V) and V(IV) ions were potentiometrically titrated. V(V) ions were reduced by standardized Fe(II) solutions in an acid medium (H_2SO_4 , H_3PO_4). V(IV) ions were

oxidized in a neutral medium by an excess of $\text{Fe}(\text{CN})_6^{3-}$ under a nitrogen flow. The resulting Fe(II) ions were then titrated by a standardized permanganate solution.

Molecular weight determination was made by light scattering and ultracentrifugation. Light-scattering experiments were carried out with monochromatic light ($\lambda = 546 \text{ nm}$) with a Fica photogoniometer. The light scattered by the solution was compared with the light scattered by benzene, the Rayleigh constant of which is well-known. The solution was clarified by preparative centrifugation (10^4 rpm during 1 h), vanadium concentration being measured afterwards. Ultracentrifuge measurements were carried out with a Beckman Model E ultracentrifuge equipped with schlieren and U.V. optics, and with a photoelectric scanner. The solvents used for the runs were pure water or LiNO_3 or $\text{HCl } 10^{-3} \text{ mol L}^{-1}$ solutions. They were slowly added and well stirred just before the runs. No flocculate was then observed under such experimental conditions, and the results do not seem to be affected by the nature of the added electrolyte.

Band centrifugations¹¹ were carried out either in a 20% sucrose $10^{-2} \text{ mol L}^{-1}$ LiNO_3 medium or in a 1.5 mol L^{-1} trichloroacetic acid medium. All the "S" values were converted into the same solvent conditions (water 20°C).¹² These corrected values do not depend on the solvent used. Distribution curves for sedimentation coefficients were extrapolated to infinite centrifugation time, all corrections for the changes in boundary shape caused by the cell and centrifugation conditions having been previously made.¹³

ESR experiments were performed on a JEOL ME 3X X-band spectrometer. Low- and high-temperature measurements were obtained by blowing nitrogen gas through the cavity. The magnetic field was measured with a proton probe NMR gauss meter. The microwave frequency was measured with a wavemeter giving an accuracy of $\pm 1 \text{ MHz}$.

Electronic spectra were performed on a Beckman MIV spectrophotometer modified in order to have a monochromatic incident light over the whole frequency range ((5×10^4) – $(5 \times 10^3) \text{ cm}^{-1}$).

- (1) A. Ditte, C. R. *Hebd. Seances Acad. Sci.*, **101**, 698 (1885).
- (2) P. Düllberg, *Z. Phys. Chem., Stoechiom. Verwandtschaftsl.*, **45**, 129 (1903).
- (3) W. Biltz, *Ber. Dtsch. Chem. Ges.*, **37**, 1098 (1904).
- (4) E. Müller, *Z. Chem. Ind. Kolloide*, **8**, 302 (1911).
- (5) J. B. Donnet, H. Zbinden, H. Benoit, M. Daume, N. Dubois, J. Pouyet, G. Scheibling, and G. Vallet, *J. Chim. Phys. Phys.-Chim. Biol.*, **47**, 52 (1950).
- (6) H. Zbinden and K. Huber, *Experientia*, **3**, 452 (1947).
- (7) U. T. Foreman, *J. Chem. Phys.*, **32**, 277 (1960).
- (8) S. Ghosh and S. D. Dhar, *Z. Anorg. Chem.*, **190**, 421 (1930).
- (9) J. Lemerle, L. Néjem, and J. Lefebvre, *J. Chem. Res., Miniprint*, 301 (1978).
- (10) J. Bullot, O. Gallais, M. Gauthier, and J. Livage, *Appl. Phys. Lett.*, **36**, 986 (1980).
- (11) J. Vinograd, R. Bruner, R. Kent, and H. Weigle, *Proc. Natl. Acad. Sci. USA*, **49**, 902 (1963).
- (12) T. Svedberg and K. O. Pedersen, "The Ultracentrifuge", Johnson Reprint Co., New York, 1960.
- (13) F. Sécheresse, J. Lemerle, and J. Lefebvre, *Bull. Soc. Chim. Fr.*, **11**, 2423 (1974).

* To whom correspondence should be addressed at the Spectrochimie du Solide.

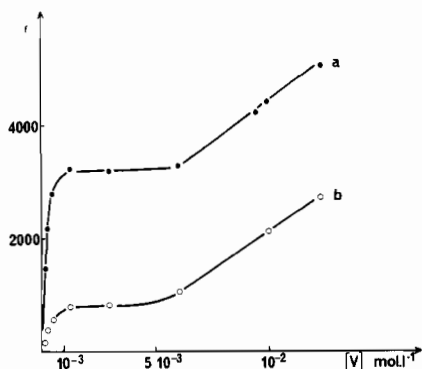


Figure 1. Molar absorption coefficient ϵ (related to one V) of polyvanadic acid as a function of vanadium concentration: (a) $\lambda = 268$ nm; (b) $\lambda = 380$ nm.

Electrical conductivity measurements have been performed on thin layers deposited from polyvanadic acid gels. Chemical analysis of this gel indicates that it is 0.5 M in vanadium and the ratio $C = [V(IV)]/[V(IV)] + [V(V)] = 0.01$. Once deposited, the layer is left at room temperature. The water adsorbed at the surface of the gel readily evaporates, and a rather hard and homogeneous coating is obtained after a few hours. The thickness of these layers was measured by optical observation of interference fringes. Gold electrodes were evaporated in a coplanar geometry on the surface of the layer. External connections were made with Ag-loaded epoxy resin (H20E Epotek). Resistance measurements were carried out by means of a 225 Keithley current source and a 616 Keithley electrometer. The sample was located in a cryostat through which temperature-controlled nitrogen gas circulates.

Results

(a) Polymerization Process. Polymerization of a vanadic acid solution spontaneously occurs upon aging. It has already been shown that it follows an autocatalytic condensation process involving two kinds of chemical species: decavanadic acid and high polymers.¹⁴ ESR experiments show that some V(IV) ions are formed during the polymerization process. Such a reduction of V(V) is due to an oxidation of both the organic ion exchanger and the water. Using an inorganic ion exchanger such as β -antimonic acid¹⁵ decreases the amount of V(V) ions and increases the polymerization rate. On the other hand, polymerization can be enhanced by adding V(IV) ions (as $VOSO_4$ up to 0.02 mol/vanadium) to the freshly prepared vanadic acid.

Molar absorbance (related to one V) in the charge-transfer region depends on the vanadium concentration. Three different concentration ranges can be seen in Figure 1 depending on whether the vanadium concentration is smaller than 10^{-3} mol L^{-1} , larger than 6×10^{-3} mol L^{-1} , or included between these two values. Such a dependence of molar absorbance vs. vanadium concentration indicates that some equilibrium occurs between different chemical species, the ratio of which depends on the total vanadium concentration. Aged polyvanadic acid solutions ($[V] \approx 0.1$ mol L^{-1}) contain a large amount of highly condensed species that can be related to the number of H^+ ions neutralized during a rapid protometric titration at pH 10. These high polymers can be isolated by preparative ultraconfiguration.⁹ Figure 2 shows that the ratio of high polymers decreases when the vanadium concentration decreases. The molar absorbance increase above $[V] \approx 6 \times 10^{-3}$ mol L^{-1} can then be related to the presence of highly condensed species, which will be called "associated species". No high polymer is observed when the vanadium concentration is smaller than 10^{-2} mol L^{-1} (Figure 1) so the question arises whether the

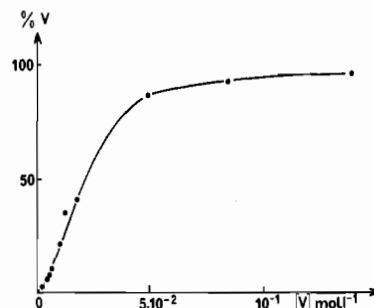


Figure 2. Relative abundance (expressed as % V) of associated species (pelleted by preparative centrifugation) as a function of vanadium concentration.

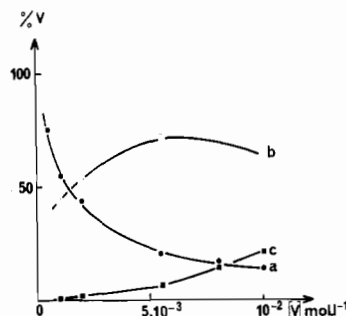


Figure 3. Relative abundance (expressed as % V) of different species in polyvanadic acid solutions as a function of vanadium concentration: (a) decavanadic species; (b) polymeric species; (c) associated species.

vanadic acid is already condensed when no pellet can be obtained by preparative ultracentrifugation (12×10^3 rpm during 1 h)?

We observed that a polyvanadic acid solution ($[V] < 10^{-2}$ mol L^{-1}) does not completely pass through a Pellicon PSAC membrane (NMWL = 1000) while under the same experimental conditions a decavanadate solution (molecular weight $M_r \approx 1000$) would completely pass through the membrane. It is then obvious that some condensed species ($M_r > 10^3$) already exist in vanadic acid solutions even when no associated species are observed. We shall call these "polymeric species". Their abundance increases with the vanadium concentration as shown in Figure 3. The chemical species that are not stopped by the membrane have been characterized by their optical spectrum and their molecular weight, $M_r = 970$. Decavanadic acid together with polymeric and associated species can be found simultaneously in aged polyvanadic acid solutions. The relative amount of each species depends on the vanadium concentration (Figure 3). Decavanadic acid predominates below 10^{-3} mol L^{-1} , associated species predominate above 2×10^{-2} mol L^{-1} , and polymeric species predominate between these two concentrations.

The molecular parameters of the "polymeric" and "associated" species have been determined by light-scattering and analytical ultracentrifuge experiments. Light scattering was performed on polyvanadic acid solutions containing less than 10^{-3} mol L^{-1} of vanadium, in a concentration range where the absorbance of the solution can be neglected. The decavanadic acid concentration is then approximately constant (6×10^{-4} mol L^{-1}) so that the solvent can be considered as a decavanadate solution. The excess of light scattered by the polymeric species has been calculated and is represented as a Zimm plot¹⁶ in Figure 4. The extrapolated value of the excess of scattered light ($C \rightarrow 0$, $\theta \rightarrow 0$) leads to a weight average molecular weight of 1.6×10^6 . No "associated species" can exist in the concentration range studied here, so

(14) J. Lemerle, L. Nĕjem, and J. Lefebvre, *J. Inorg. Nucl. Chem.*, **42**, 17 (1980).

(15) J. Lemerle, *Rev. Chim. Miner.*, **9**, 863 (1972).

(16) B. H. Zimm, *J. Phys. Chem.*, **16**, 260 (1948).

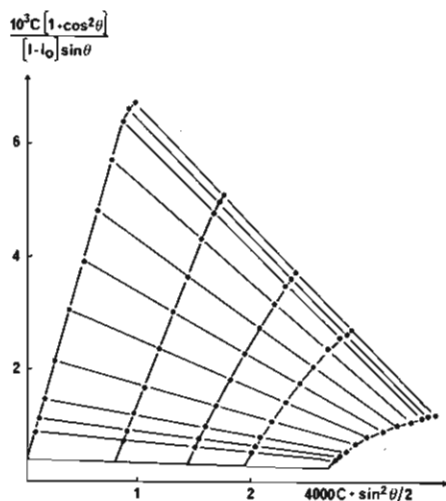


Figure 4. Zimm plot¹⁶ for dilute polyvanadic acid solutions; C = vanadium concentration (polymeric species only), I = intensity of the light scattered by the sol at an angle θ , and I_0 = intensity of the light scattered by the solvent at the same angle θ . Four vanadium concentrations have been studied, corresponding respectively to polymer concentrations $[V] = 6.25 \times 10^{-4}$, 4.85×10^{-4} , 3.5×10^{-4} , and 2×10^{-4} mol L⁻¹. The fifth curve, corresponding to $C = 0$, was obtained by extrapolation of the preceding measurements.

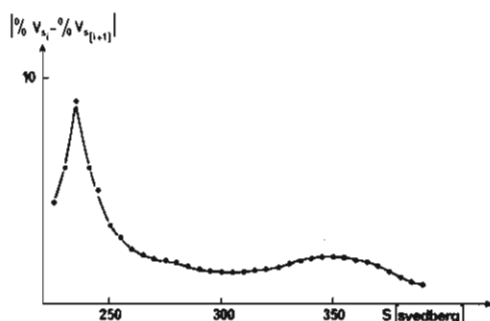


Figure 5. Distribution of apparent sedimentation coefficient S of high-condensed species (polymeric and associated species) of polyvanadic acid ($[V] \approx 5 \times 10^{-2}$ mol L⁻¹). $|\% V_{S_i} - \% V_{S_{i+1}}|$ is the relative abundance (expressed in percent) of vanadium in the condensed species having a sedimentation coefficient in the $S_i - S_{i+1}$ range.

the molecular weights measured in these experiments correspond to "polymeric species" only.

Analytical ultracentrifuge experiments have been performed in the concentration range where associated species are also observed (10^{-3} mol L⁻¹ < $[V]$ < 0.1 mol L⁻¹). Conventional centrifugation exhibits two peaks sedimenting with a great velocity. The resolution of these peaks increases when the vanadium concentration decreases. The fast component appears to be less homogeneous than the slow one as can be seen on the apparent sedimentation distribution curve (Figure 5). The smaller sedimentation velocity is attributed to the "polymeric species" while the larger one is related to the "associated species". Variation of the apparent sedimentation coefficient vs. vanadium concentration is plotted in Figure 6. S values obtained by band centrifugation are close to those deduced from conventional ultracentrifugation. A single sedimentation peak is observed for vanadium concentrations up to 10^{-3} mol L⁻¹. It can be attributed to polymeric species only and is in good agreement with the results of ultrafiltration.

Polyvanadic acid solutions exhibit a Newtonian behavior when the vanadium concentration remains quite small ($[V] < 10^{-2}$ mol L⁻¹). Their intrinsic viscosity is referred to as the polymer viscosity (the excess of viscosity due to the decavanadic species is neglected) and corresponds to 145 mL g⁻¹ (Figure 7) at room temperature (20 °C). These solutions

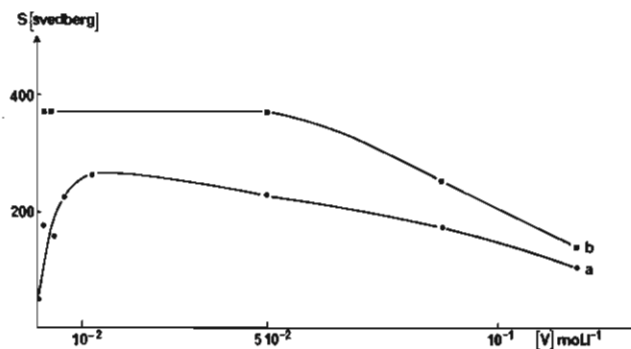


Figure 6. Changes in apparent sedimentation coefficient S vs. vanadium concentration for (a) the polymeric species and (b) the associated species.

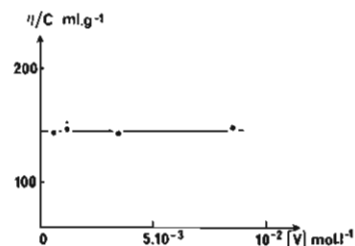


Figure 7. Changes in reduced viscosity η/C of dilute polyvanadic acid solutions vs. vanadium concentration.



Figure 8. Electron micrograph of polyvanadic acid gel showing the polymeric texture of the condensed species.

become pseudoplastic when the vanadium concentration becomes larger than 10^{-2} mol L⁻¹. Above 0.2 mol L⁻¹, they exhibit a yield point that increases with the vanadium concentration.

Electron micrographs of polyvanadic acid solutions ($[V] = 10^{-2}$ mol L⁻¹) were taken with a JEOL Jem 100C apparatus. A drop of the colloidal solution was deposited onto a 200-mesh copper grill, dried in air, and then observed under the electron microscope. These experiments show (Figure 8) that the gel is made of entangled fibers, about 1 μ long and 100 Å in diameter.

(b) Electron Spin Resonance. The ESR spectra of a polyvanadic acid gel ($[V] = 0.1$ mol L⁻¹) are shown in Figure 9. At room temperature, it exhibits eight lines due to the hyperfine coupling of one unpaired electron ($S = 1/2$) with the nuclear spin ($I = 1/2$) of one ⁵¹V. It can then be described with the usual isotropic spin Hamiltonian

$$\mathcal{H}_{iso} = g_{iso}\beta HS + A_{iso}SI$$

An intensity distribution is observed among these hyperfine lines. Their width appears to depend on the corresponding

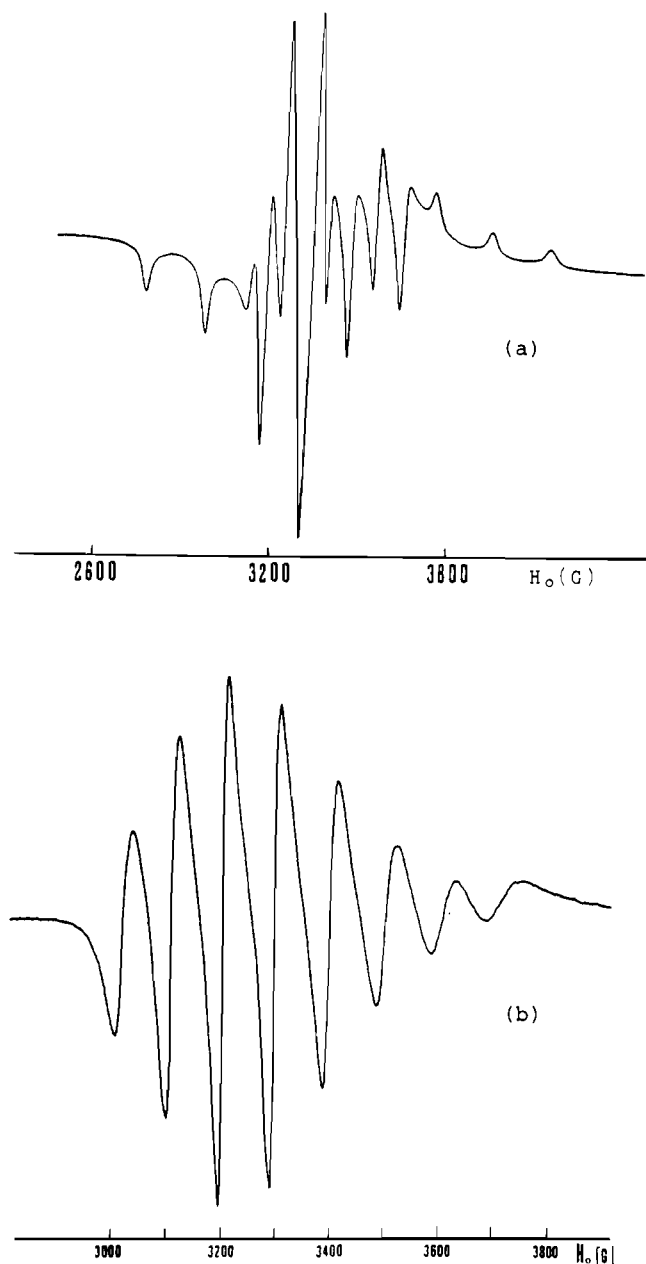


Figure 9. ESR spectra of a polyvanadic acid gel at (a) 77 K and (b) 300 K.

nuclear spin quantum number. Such a behavior is typical of a fast tumbling motion of the molecular species under study.¹⁷

Due to this molecular motion, the isotropic ESR parameters vary slightly with temperature.¹⁸ They were determined by a computer simulation taking into account second-order perturbation terms. The best fit between simulated and experimental spectra gives $g_{iso} = 1.954$ and $A_{iso} = 115$ G. A well-resolved frozen-solution ESR spectrum is observed at low temperature. Both parallel and perpendicular features can be seen on the spectrum showing that V(IV) ions are in an axially distorted ligand field. Such a spectrum can be described by the spin Hamiltonian

$$\mathcal{H} = g_{\parallel}\beta H_z S_z + g_{\perp}\beta(H_x S_x + H_y S_y) + A_{\parallel}S_z I_z + A_{\perp}(S_x I_x + S_y I_y)$$

where z is taken along the main axis of g and A tensors. A computer simulation was again necessary in order to get ac-

Table I. ESR Parameters of V⁴⁺

compd	g_{\parallel}	g_{\perp}	A_{\parallel} , G	A_{\perp} , G	ref
polyvanadic acid	1.935	1.981	-200	-75	this work
VO ²⁺ (H ₂ O) ₆	1.931	1.978	-205	-76	19
V ₂ O ₅ , single cryst	1.913	1.985	-176	-66	30

Table II. Electronic Transitions in Polyvanadic Acid Gels

$\bar{\nu}$, cm ⁻¹	assignt	ϵ^a
52 000	charge transfer	8500
37 300	charge transfer	8250
26 200	charge transfer	5000
15 500	$b_2 \rightarrow a_1$	21
14 200	$b_2 \rightarrow b_1$	18
12 800	$b_2 \rightarrow e$	17
7 100	intervalence	69
6 600	charge transfer	72

^a ϵ is referred to the total vanadium concentration. These values of ϵ are calculated for a sol having a vanadium concentration of 0.1 mol L⁻¹ and a [V(IV)]/[V(IV)] + [V(V)] ratio of 0.14.

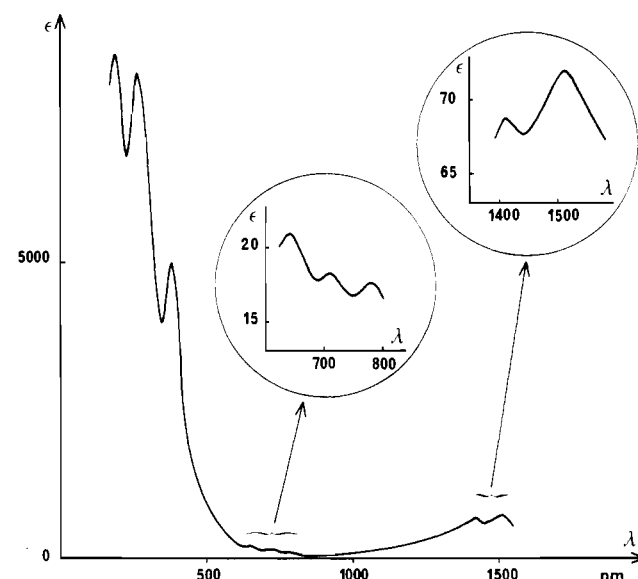


Figure 10. Electronic spectrum of a polyvanadic acid solution. ϵ is referred to total vanadium concentration. In this solution [V(IV)]/[V(V)] = 0.14.

curate values of the ESR parameters. These values are reported in Table I.

(c) Electronic Spectra. Colloidal solutions of polyvanadic acid have an orange color when freshly prepared. Their electronic spectra only exhibit a shoulder around 38 000 cm⁻¹. The color then gradually turns to red upon aging while the solution becomes more and more viscous. A dark red gel is finally obtained, the optical spectrum of which is shown in Figure 10. Several absorption bands are observed. Their positions are reported in Table II together with the corresponding molar absorption coefficients (expressed vs. total vanadium concentration). All the positions of the transitions are independent of the V(IV) ratio in the gel. The two bands on the red side of the spectrum (6600 and 7100 cm⁻¹) can presumably be attributed to intervalence transfers between V(IV) and V(V) ions. Their molar absorption coefficients linearly increase up to 100 for a [V(IV)]/[V(V)] ratio of 0.25 and then decreases below this value.

As already reported for vanadyl ions in aqueous solutions, the weak transitions in the 12 000–16 000 cm⁻¹ region should correspond to forbidden d–d transitions.^{19–21} Their intensity

(17) R. Wilson and D. Kivelson, *J. Chem. Phys.*, **44**, 154 (1966).

(18) P. Tougné, A. P. Legrand, C. Sanchez, and J. Livage, *J. Phys. Chem. Solids*, **42**, 101 (1981).

(19) C. J. Ballhausen and H. B. Gray, *Inorg. Chem.*, **1**, 111 (1962).

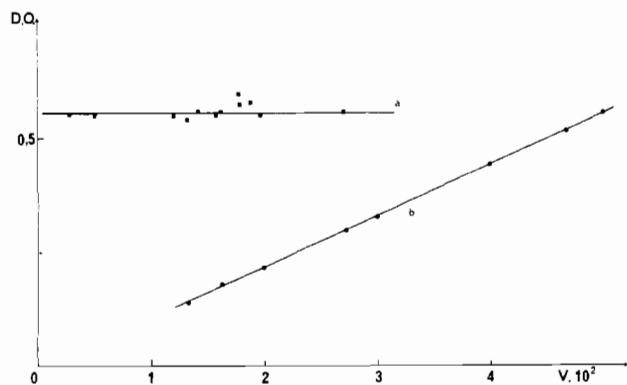


Figure 11. Plot of the absorption of polyvanadic acid in the charge-transfer region ($\bar{\nu} = 26\,200\text{ cm}^{-1}$) vs. V(IV) concentration (curve a) or V(V) concentration (curve b) (length of the cell $2 \times 10^{-3}\text{ cm}$).

(related to the total Vanadium concentration) strongly depends on the amounts of V(IV) ions in the gel. They disappear when the polyvanadic acid is oxidized by hydrogen peroxide in an acidic medium. The apparent total intensity of these transitions is more important than the expected intensity for V(IV) ions in aqueous solutions. These bands actually appear on the red side of the intense transition located around $26\,000\text{ cm}^{-1}$ (described as a charge-transfer band). If we measure the difference between two gels of different known V(IV) concentrations, the molar absorption coefficient calculated is then close to that of V(IV) in aqueous solutions ($\epsilon \sim 7$).

The very intense absorption in the UV region can be attributed to symmetry-allowed charge-transfer transitions of an electron from the oxygen π orbitals to the ligand field vanadium d levels. The intensity of the most energetic transition ($52\,000\text{ cm}^{-1}$) depends on the amount of V(IV) ions in the gel and could be related to charge-transfer transition to V(IV) levels.

Some controversy remains about the optical absorption of vanadyl solutions around $26\,000\text{ cm}^{-1}$. Ballhausen and Gray suggest a d-d transition¹⁹ while Selbin et al. claim that it should rather correspond to a charge transfer between oxygen and V(IV).^{20,21} In the case of polyvanadic acid gels, our own experiments suggest that the optical absorption at $26\,200\text{ cm}^{-1}$ arises from charge transfer between oxygen and V(V) ions. Its intensity varies linearly with the V(V) concentration in the same way as the $37\,300\text{-cm}^{-1}$ transition, which can unambiguously be attributed to charge transfer (Figure 11). On the other hand, the three d-d bands between $12\,000$ and $16\,000\text{ cm}^{-1}$ are related to the V(IV) concentration and disappear when the gel is oxidized by H_2O_2 while the $26\,200\text{-cm}^{-1}$ transition does not vary noticeably.

(d) Electrical Conductivity Measurements. Colloidal polyvanadic acid solutions can be deposited as thin layers on a glass substrate.¹⁰ Electrical conductivity measurements have been performed on these layers. They exhibit semiconducting properties due to the thermally activated hopping of unpaired electrons between V(IV) and V(V) ions. Figure 12 shows the temperature dependence of conductivity from room temperature down to 100 K . The measured conductivity at 300 K is $\sigma = 0.6\ \Omega^{-1}\text{ cm}^{-1}$, a very high value indeed when compared with known data for V_2O_5 crystals ($\sigma \approx 10^{-2}\ \Omega^{-1}\text{ cm}^{-1}$)^{22,23} or amorphous V_2O_5 thin films (10^{-4} – $10^{-6}\ \Omega^{-1}\text{ cm}^{-1}$).²⁴ On the

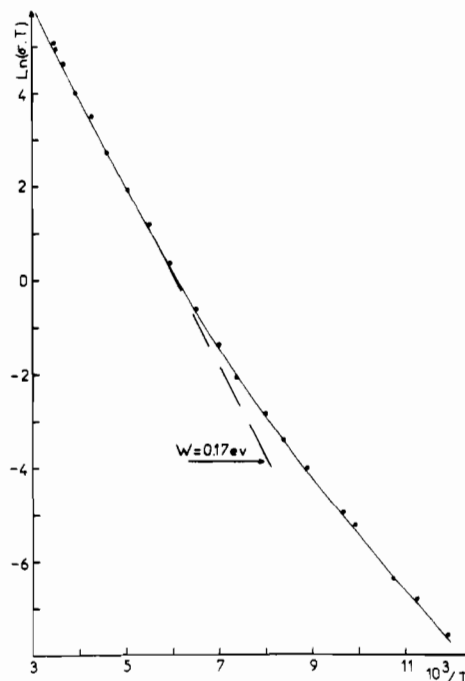


Figure 12. Temperature dependence of the dc conductivity of thin layers deposited from polyvanadic acid gels.

other hand, these results agree with those previously reported for other vanadium pentoxide gels obtained by pouring molten V_2O_5 into water ($\sigma \approx 1\ \Omega^{-1}\text{ cm}^{-1}$).¹⁰ Their conductivity was slightly larger, but the $[\text{V(IV)}]/[\text{V(V)}]$ ratio was also higher (6%) than that in our polyvanadic acid gels (1%). dc conductivity quickly decreases when the temperature decreases, and a nonlinear plot of $\ln(\sigma T)$ vs. T^{-1} is obtained. Such a behavior is typical of amorphous transition-metal oxides.²⁵

Discussion

(a) Vanadium Coordination. V(V) ions are considered to be somewhat large for tetrahedral coordination to oxygen and somewhat small for octahedral coordination. The possibility of very irregular structures therefore arises. Anhydrous metavanadates are made of VO_4 tetrahedra while hydrated ones exhibit infinite chains of VO_5 polyhedra.²⁶ Decavanadate ions, $\text{V}_{10}\text{O}_{28}^{6-}$, are made of ten VO_6 octahedra.²⁷ Vanadium ions in orthorhombic V_2O_5 crystals are surrounded by five oxygens.²⁸ The question therefore arises about vanadium coordination in the colloidal polyvanadic acid.

These compounds lose their water when heated above $300\text{ }^\circ\text{C}$, leading to crystalline orthorhombic V_2O_5 .²⁹ This suggests that some correlation may exist between vanadium coordination in both compounds. On the other hand, it seems worthwhile to notice that the ESR parameters measured on the gels are quite different from those reported for crystalline or amorphous V_2O_5 ^{30–32} (Table I). This suggests that V(IV) ions in the gel are surrounded by six oxygen ions rather than

- (20) J. Selbin, T. R. Ortolano, and F. J. Smith, *Inorg. Chem.*, **2**, 1315 (1963).
 (21) T. R. Ortolano, J. Selbin, and S. P. McGlynn, *J. Chem. Phys.*, **41**, 262 (1964).
 (22) J. H. Perlstein, *J. Solid State Chem.*, **3**, 217 (1971).
 (23) J. Haemers, E. Baetens, and J. Vennik, *Phys. Status Solidi A*, **20**, 381 (1973).
 (24) F. P. Koffyberg and F. A. Benko, *Philos. Mag. B*, **38**, 357 (1978).

- (25) I. G. Austin and N. F. Mott, *Adv. Phys.*, **18**, 41 (1969).
 (26) H. T. Evans, *Z. Kristallogr., Kristallgeom., Kristallphys., Kristallchem.*, **114**, 257 (1960).
 (27) A. G. Swallow, F. R. Ahmed, and W. H. Barnes, *Acta Crystallogr.*, **21**, 397 (1966).
 (28) H. G. Backmann, F. R. Ahmed, and W. H. Barnes, *Z. Kristallogr., Kristallgeom., Kristallphys., Kristallchem.*, **115**, 110 (1961).
 (29) M. Michaud, M. C. Leroy, and J. Livage, *Mater. Res. Bull.*, **11**, 1425 (1976).
 (30) E. Gillis and E. Boesman, *Phys. Status Solidi*, **14**, 337 (1966).
 (31) A. Kahn, J. Livage, and R. Collongues, *Phys. Status Solidi A*, **26**, 175 (1974).
 (32) N. Gharbi, C. R'kha, D. Ballutaud, M. Michaud, J. Livage, J. P. Audière, and G. Schiffmacher, *J. Non-Cryst. Solids* **46**, 247 (1981).

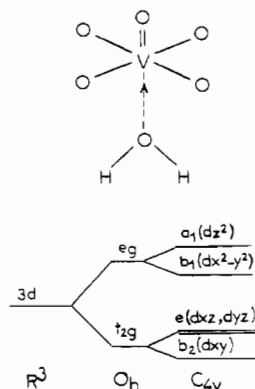


Figure 13. V(IV) coordination in polyvanadic acid gels and d-orbital splitting in a C_{4v} ligand field according to ref 19.

five. They must be strongly solvated by water molecules. Our ESR experiments indicate that V(IV) lies in an axially distorted ligand field. The measured g and A values being quite similar to those reported by Gray and Ballhausen for $VO^{2+}(H_2O)_5$,¹⁹ we may assume that vanadium is surrounded by six oxygen ions with a short $V=O$ double bond. It seems reasonable to suggest that the sixth coordination site, opposite to the vanadyl group, might be occupied by a water molecule. This H_2O molecule would then be liberated upon heating, leaving a five-coordinated vanadium as in crystalline V_2O_5 .

Taking this picture as a reasonable model, we then assume that V(IV) ions are surrounded by a C_{4v} ligand field as shown in Figure 13. The g values indicate that the unpaired electron lies in a orbitally nondegenerated b_2 (d_{xy}) orbital as in $VO^{2+}(H_2O)_5$. We may then use the MO calculations of Ballhausen and Gray¹⁹ in order to extract the ligand field parameters. The three d-d transitions correspond to

$${}^2E \leftarrow {}^2B_2 \quad 12800 \text{ cm}^{-1} \quad E = -3Ds + 5Dt$$

$${}^2B_1 \leftarrow {}^2B_2 \quad 14200 \text{ cm}^{-1} \quad E = 10Dq$$

$${}^2A_1 \leftarrow {}^2B_2 \quad 15500 \text{ cm}^{-1} \quad E = 10Dq - 4Ds - 5Dt$$

This leads to

$$Dq = 1420 \text{ cm}^{-1} \quad Ds = -2014 \text{ cm}^{-1}$$

$$Dt = 1351 \text{ cm}^{-1}$$

Dq corresponds to the cubic crystal field component while Ds and Dt specify the degree of tetragonal distortion of the ligand field.¹⁹

The ground-state wave function of the unpaired electron can be expressed as

$$|b_2\rangle = a|d_{xy}\rangle + a'|\varphi b_2\rangle$$

where $|\varphi b_2\rangle$ represents the ligand orbital combination having the B_2 symmetry.

The hyperfine parameters corresponding to a d_{xy} unpaired electron in a C_{4v} ligand field can be approximately expressed as

$$A_{||} = P[-\frac{4}{7}a^2 - K + (g_{||} - g_e) + \frac{3}{7}(g_{\perp} - g_e)]$$

$$A_{\perp} = P[\frac{3}{7}a^2 - K + \frac{1}{4}(g_{\perp} - g_e)]$$

where $g_e = 2.0023$ is the free-electron g factor, K is the isotropic Fermi contact term, and $P = g_e g_n \beta_e \beta_n \langle r^{-3} \rangle$. P depends on the effective charge carried by the vanadium ion. $P = 0.0128 \text{ cm}^{-1}$ corresponding to the vanadyl ion is usually taken for such compounds, leading to $a^2 = 0.53$. Optical absorption and ESR experiments show that the polyvanadic acid gel can be considered as a class II mixed-valence compound according to the classification proposed by Robin and Day.³³

(b) Electron Delocalization. Electron transfer between metallic ions in different oxidation states is usually observed in class II mixed-valence compounds. It occurs through a hopping process, which may be either optically or thermally activated. According to Hush³⁴ and Mott,²⁵ a relationship can be found between the optical E_{opt} and thermal E_{th} activation energies:

$$\frac{1}{4}E_{opt} = E_{th} + |J| - J^2/E_{opt}$$

where J represents the transfer integral between both metallic ions.

The optical activation energy can be deduced from electronic spectra of mixed-valence compounds where low-energy intervalence bands are observed. In our compounds, these bands result from transitions within a ground vibronic manifold arising from the coupling between V(IV) and V(V) ions. They occur at 6600 and 7100 cm^{-1} , in the red part of the spectrum (Table I), leading to the optical activation energy

$$E_{opt} \approx 0.87 \text{ eV}$$

The thermal activation energy is usually more difficult to measure. A thermally activated hopping could lead to a broadening of the ESR line width with temperature. Such a broadening is not observed in our ESR spectra in the temperature range 4–200 K, showing that the hopping frequency remains smaller than the linewidth ΔH expressed in frequency units:

$$\nu_h < \Delta H = 60 \text{ MHz}$$

Above 200 K, the fibers forming the gel undergo a Brownian motion, which leads to a modification of the shape and line width of the ESR spectrum. An analysis of the electron hopping becomes therefore impossible, but anyway, up to 400 K, no broadening due to electron mobility seems to occur.

The dc conductivity measurements made on thin layers deposited from polyvanadic acid solutions could on the other hand give more information about the thermally activated hopping process. As seen in Figure 12 a curved plot of $\ln(\sigma T)$ vs. T^{-1} is obtained. Such a behavior is encountered in all amorphous V_2O_5 thin films^{24,35} or V_2O_5 -containing glasses.³⁶ So far, most experimental data have been interpreted in terms of the small-polaron theory. According to Mott²⁵ the conductivity is then given by

$$\sigma = [\nu_0 e^2 c(1-c)/kTR] \exp(-2\alpha R) \exp(-E_{th}/kT)$$

where ν_0 is a phonon frequency, α the rate of the wave function decay, and R the average hopping distance. e and k have their usual meanings, and C corresponds to the $[V(IV)]/[V(V)]$ ratio. In our case $C = 0.01$. The thermal activation energy can be extracted from the high-temperature-range data, where the $\ln(\sigma T)$ vs. T^{-1} plot may be approximated by a straight line (300–180 K). This gives

$$E_{th} = 0.17 \pm 0.01 \text{ eV}$$

Below 180 K, the theory predicts that E_{th} drops continuously down to $\frac{1}{2}W_d$, where W_d represents the disorder energy due to the random structure of the medium.²⁵ We shall not give here a detailed analysis of the dc conductivity measurements but only compare the room-temperature thermal activation

(33) M. B. Robin and P. Day, *Adv. Inorg. Chem. Radiochem.*, **10**, 247 (1967).

(34) N. S. Hush, *Prog. Inorg. Chem.*, **8**, 391 (1967).

(35) T. Allersma, R. Hakim, T. N. Kennedy, and J. D. Mackenzie, *J. Chem. Phys.*, **46**, 154 (1967).

(36) L. Murański, C. H. Chung, and J. D. Mackenzie, *J. Non-Cryst. Solids*, **32**, 91 (1979).

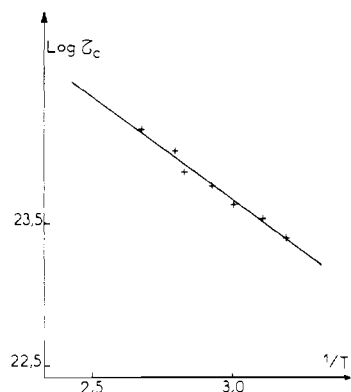


Figure 14. Correlation time τ_c of the Brownian motion of polyvanadic acid fibers vs. temperature T .

energy $E_{th} = 0.17$ eV to the optical activation energy $E_{opt} = 0.87$ eV in order to evaluate the transfer integral

$$J = 0.05 \text{ eV} \approx 400 \text{ cm}^{-1}$$

(c) Brownian Motion of the Polymer. An intensity distribution is observed among the eight hyperfine lines of the room-temperature ESR spectrum of a polyvanadic acid gel (Figure 9). The line width depends on the nuclear spin quantum number. This is typical of a fast-tumbling motion of V(IV) ions, which can be analyzed according to Kivelson's theory.¹⁷ In the fast-tumbling limit the line width ΔH of each hyperfine line can be expressed as a function of the nuclear spin quantum number M :

$$\Delta H(M) = \alpha + \beta M + \gamma M^2 + \delta M^3$$

The four coefficients α , β , γ , and δ depend on the magnetic ESR tensors \mathbf{g} and \mathbf{A} , the microwave frequency ω , and two temperature-dependent quantities, namely, the residual line width α_r and the correlation time of the motion τ_c .

The static parameters g and A can be deduced from the frozen-solution spectrum (Table I). The microwave frequency is measured with a wavemeter. The dynamic parameters α_r and τ_c can be calculated by minimization of the expression

$$F = \sum_M [\Delta H_{\text{exptl}}(M) - \Delta H_{\text{th}}(M)]^2$$

where $\Delta H_{\text{exptl}}(M)$ is the experimental width of the Lorentzian hyperfine line corresponding to the nuclear quantum number M . This line width can be determined by measuring accurately the width of the most intense line ($M = -3/2$). The relative widths of the other lines are then deduced by comparing their intensities. $\Delta H_{\text{th}}(M)$ is the theoretical line width calculated with a given value of α_r and τ_c . Minimization is performed over these two temperature-dependent parameters. ESR spectra were analyzed over a temperature range where molecular motion corresponds to the fast-tumbling case, i.e., from 20 up to 100 °C. A variation of α_r and τ_c with temperature can then be established.

In this temperature range, α_r increases from 8.7 G at 20 °C up to 16.7 G at 100 °C while τ_c decreases from 1.2×10^{-10} s down to 7×10^{-11} s. These values of τ_c are about 1 order of magnitude larger, than those previously reported for VO-(H₂O)₅²⁺ in water solutions,⁴¹ suggesting that V(IV) ions are linked to relatively large molecular species. It is too fast anyway to be attributed to the motion of the polymer as a whole. It must correspond to local motions around a chemical bond as observed with organic polymers.^{37,38}

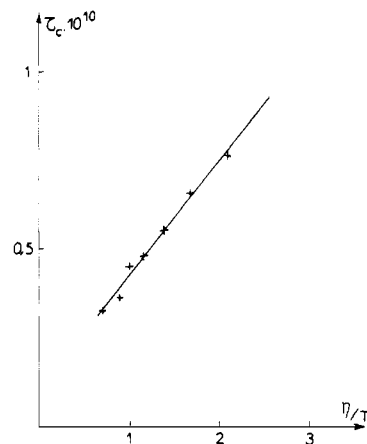


Figure 15. Correlation time τ_c of the Brownian motion of polyvanadic acid fibers vs. the water viscosity η .

The temperature dependence of the correlation time τ_c can be fitted with an exponential relationship (Figure 14):

$$\tau_c = \tau_0 \exp(-E/kT)$$

The activation energy E of the V(IV) motion can then be deduced from the slope of the curve:

$$E = 1.7 \text{ kcal mol}^{-1} \quad \tau_0 = 10^{-12} \text{ s}$$

These values agree with those previously found in the literature for molecular reorientations around a C-C bond in organic polymers.^{37,38}

The V(IV) spin-label motion can also be correlated to the viscosity η of the water in which the colloidal polyvanadic acid is dispersed. A linear dependence of τ_c with η/T is obtained (Figure 15) according to

$$\tau_c = 4\pi \frac{r^3 \eta}{3kT} + \tau_0$$

T is the absolute temperature and r the equivalent hard-sphere radius associated with the V(IV) motion. A value of $r = 4.2$ Å can be deduced from the slope of the curve. This radius is slightly larger than the shortest V-V distance in orthorhombic V₂O₅ (3.2 Å), showing that the fibers undergo only local motions. The Debye equation used here is of course only valid for isotropically tumbling large spherical molecules. Strictly speaking, it should not be used for local motions in polymeric species. Nevertheless, it gives an estimation of the free volume in which the V(IV) ion is moving and is often used by polymer chemists.^{37,38}

These ESR results about V(IV) motion can be correlated to those obtained by light-scattering experiments showing that the polyvanadic acid colloids are polydispersed coils rather than rods. The unusual shape of the Zimm plot (Figure 4) relative to the polymeric species in solution can be discussed in terms of electrostatic interactions. The curve $C/I_{\theta \rightarrow 0} = f(c)$ has a slightly negative slope related to a solvent-segment interaction slightly weaker than a segment-segment interaction. Under these conditions, the particle is coiled when the polymer concentration increases and the dissymmetry ratio of scattered light decreases. If an indifferent electrolyte is added to the solution, the segment-segment interaction can be weakened and the angular distribution of the light scattered does not depend on the polymer concentration. In our case, we have considered decavanadic species in equilibrium with polymeric species as the solvent. The decavanadic acid is only slightly dissociated, and this is not sufficient to balance efficiently the charge effect. If LiNO₃ is added to the polyvanadic solutions (only small amounts can be added without flocculation), the dissymmetry ratio is enhanced for the upper concentration,

(37) M. C. Lang, C. Noel, and A. P. Legrand, *J. Polym. Sci.*, **15**, 1329 (1977).

(38) H. Homel, L. Facchini, A. P. Legrand, and J. Lecourtier, *Eur. Polym. J.*, **14**, 803 (1978).

Table III. Angular Distribution of Scattered Light

θ , deg	$P(\theta)$ - (exptl)	$P(\theta)$ - (calcd) ^a	θ , deg	$P(\theta)$ - (exptl)	$P(\theta)$ - (calcd) ^a
30	0.455	0.456	105	0.083	0.082
37.5	0.357	0.355	120	0.070	0.069
45	0.278	0.278	135	0.063	0.061
60	0.186	0.185	142.5	0.058	0.057
75	0.131	0.131	150	0.057	0.056
90	0.102	0.102			

^a Coils, $(F^2)^{1/2} = 475$ nm.

but the extrapolated value of $C_{C \rightarrow 0}/I_{\theta \rightarrow 0}$ and extrapolated angular distribution of the light scattered are not modified. So, we can consider that the extrapolated values used for calculations are significant. The angular distribution of the light scattered fits with coil-shaped particles $(\langle r^2 \rangle)^{1/2} = 475$ nm (Table III), in good agreement with the Brownian motion results. The molecular weight of the nonassociated species can also be calculated from the ultracentrifugation data, with use of the relationship available for flexible linear particles³⁹

$$M = \left(\frac{\eta N}{\Phi^{1/3} P^{-1}} \right)^{3/2} \frac{s_0^{3/2} [\eta]^{1/2}}{10(1 - \bar{V}\rho)^{3/2}}$$

where η = solvent viscosity, N = Avogadro's constant, s_0 = sedimentation velocity for infinite dilution, $[\eta]$ = intrinsic viscosity of the solute, \bar{V} = specific volume of the solute, and ρ = density of the solvent. $\Phi^{1/3} P^{-1}$ is taken to be equal to 2.5×10^6 . This term was originally evaluated for polymers that

(39) L. Mandelkern and P. J. Flory, *J. Chem. Phys.*, **20**, 212 (1952).

are homogeneous with regard to the molecular weight. Validity of this treatment was tested for many systems by Mandelkern.⁴⁰ The average molecular weight of the polymeric species is found to be equal to 2.35×10^6 , a value close to that determined by light-scattering experiments. The increase of the apparent sedimentation velocity with increasing concentrations for high dilutions can be discussed in terms of equilibrium displacement. When the concentration increases, the polymerization equilibrium is shifted toward the polymeric species and the average molecular weight increases, leading to an enhanced sedimentation velocity. For high concentrations, the equilibrium is shifted toward the polymeric species and the sedimentation is governed by the hydrodynamic effect.

These conclusions showing that polyvanadic acid colloids are polydispersed coils do not agree with some previous studies considering that colloidal vanadium pentoxide particles were rod shaped.⁵⁻⁷ Such a rod-shaped model was taken in order to interpret the hydrodynamic properties of colloidal solutions, but it already did not agree very well with streaming birefringence experiments and the Kerr effect, and the discrepancies were then attributed to the presence of "molecular species" in the solution.

Acknowledgment. The authors wish to thank R. Morineau for electrical conductivity measurements.

Registry No. Vanadic acid, 11140-69-5; decavanadic acid, 12273-60-8.

(40) L. Mandelkern, W. R. Krigbaum, M. A. Scheraga, and P. J. Flory, *J. Chem. Phys.*, **20**, 1392 (1952).

(41) M. M. Iannuzzi, C. P. Kubiak, and P. H. Rieger, *J. Phys. Chem.*, **80**, 541 (1976).

Contribution from the Department of Chemistry, The University of Texas at Arlington, Arlington, Texas 76019, and the Central Research Institute for Chemistry, Hungarian Academy of Sciences, H-1515 Budapest, Hungary

Kinetics and Mechanism of the Oxygenation of Bis(dimethylglyoximato)cobalt(II) in Methanol

L. I. SIMÁNDI,*^{1a,b} C. R. SAVAGE,^{1b} Z. A. SCHELLY,*^{1b} and S. NÉMETH^{1c}

The oxygenation of bis(dimethylglyoximato)cobalt(II) (cobaloxime(II), Cox) has been studied by the stopped-flow technique. A new experimental method, based on the in situ preparation of the complex, has been developed to eliminate the necessity of anaerobic work. The oxygenation of cobaloxime(II) consists of three distinct stages: (1) formation of μ -peroxy-dicobaloxime(III), $\text{Cox}(\text{O}_2)\text{Cox}$, in a rapid process, followed by (2) its slower disproportionation to μ -superoxo-dicobaloxime(III), $\text{Cox}(\text{O}_2)\text{Cox}^+$, and stable cobaloxime(III) and (3) solvolytic decomposition of $\text{Cox}(\text{O}_2)\text{Cox}^+$ to cobaloxime(III). At Hdmg^- to cobalt(II) ratios of 4:1 and higher, the μ -peroxy complex produces a transient maximum in the stopped-flow traces recorded at 440-465 nm. The spectral changes necessary for this are ascribed to the presence of a μ -peroxy species containing unidentate Hdmg^- coordinated in its two axial positions. The kinetics of the individual stages have been studied, and their mechanisms are discussed. Numerical values of the rate and equilibrium constants involved are reported.

Introduction

Bis(dimethylglyoximato)cobalt(II), $\text{Co}(\text{Hdmg})_2$, often referred to as cobaloxime(II), has been extensively studied as a vitamin B₁₂ model compound.²⁻⁵ Cobaloxime(II) derivatives have been found to react with organic halides,⁴⁻⁶ molecular

hydrogen,⁷⁻¹¹ and dioxygen,¹² which makes them potentially important homogeneous catalysts. The activation of H₂ has been investigated in detail,^{10,11} and some systems showing catalytic behavior have been reported,^{10,13-15} although the

- (1) (a) On leave of absence from the Central Research Institute for Chemistry, Hungarian Academy of Sciences, Budapest. (b) The University of Texas at Arlington. (c) Central Research Institute for Chemistry.
 (2) Schrauzer, G. N. *Acc. Chem. Res.* **1968**, *1*, 97-103.
 (3) Schrauzer, G. N. *Angew. Chem.* **1976**, *88*, 465-475.
 (4) Schrauzer, G. N. *Pure Appl. Chem.* **1973**, *33*, 545-565.
 (5) Pratt, J. M.; Craig, P. J. *Adv. Organomet. Chem.* **1973**, *11*, 331-446.
 (6) Schneider, P. W.; Phelan, P. F.; Halpern, J. *J. Am. Chem. Soc.* **1969**, *91*, 77-81.

- (7) Schrauzer, G. N.; Windgassen, R. J.; Kohnle, *Chem. Ber.* **1965**, *98*, 3324-3333.
 (8) Simándi, L. I.; Szeverényi, Z.; Budo-Záhonyi, E. *Inorg. Nucl. Chem. Lett.* **1975**, *11*, 773-777.
 (9) Simándi, L. I.; Szeverényi, Z.; Budo-Záhonyi, E. *Inorg. Nucl. Chem. Lett.* **1976**, *12*, 237-241.
 (10) Simándi, L. I.; Budo-Záhonyi, E.; Szeverényi, Z.; Németh, S. *J. Chem. Soc., Dalton Trans.* **1980**, 276-283.
 (11) Chao, T. H.; Espenson, J. H. *J. Am. Chem. Soc.* **1978**, *100*, 129-133.
 (12) Schrauzer, G. N.; Lee, L. P. *J. Am. Chem. Soc.* **1970**, *92*, 1551-1557.
 (13) Ohgo, Y.; Takeuchi, S.; Yoshimura, J. *Bull. Chem. Soc. Jpn.* **1971**, *44*, 283-285, 583.